Am J Physiol Heart Circ Physiol 293: H284–H291, 2007.
First published March 8, 2007; doi:10.1152/ajpheart.00128.2007.

Hypertrophic and dilated cardiomyopathy mutations differentially affect the molecular force generation of mouse α-cardiac myosin in the laser trap assay

Edward P. Debold,[1] J. P. Schmitt,[2] J. B. Patlak,[1] S. E. Beck,[1] J. R. Moore,[3] J. G. Seidman,[4] C. Seidman,[4,5,6] and D. M. Warshaw[1]

[1]*Department of Molecular Physiology and Biophysics, University of Vermont, Burlington, Vermont;* [2]*Institute of Pharmacology and Toxicology, University of Würzburg, Würzburg, Germany;* [3]*Department of Physiology and Biophysics, Boston University School of Medicine, Boston;* [4]*Department of Genetics and Howard Hughes Medical Institute, Harvard Medical School, Boston; and* [5]*Cardiovascular Division and* [6]*Howard Hughes Medical Institute, Brigham and Women's Hospital, Boston, Massachusetts*

Submitted 31 January 2007; accepted in final form 3 March 2007

Debold EP, Schmitt JP, Patlak JB, Beck SE, Moore JR, Seidman JG, Seidman C, Warshaw DM. Hypertrophic and dilated cardiomyopathy mutations differentially affect the molecular force generation of mouse α-cardiac myosin in the laser trap assay. *Am J Physiol Heart Circ Physiol* 293: H284–H291, 2007. First published March 8, 2007; doi:10.1152/ajpheart.00128.2007.—Point mutations in cardiac myosin, the heart's molecular motor, produce distinct clinical phenotypes: hypertrophic (HCM) and dilated (DCM) cardiomyopathy. Do mutations alter myosin's molecular mechanics in a manner that is predictive of the clinical outcome? We have directly characterized the maximal force-generating capacity (F_{max}) of two HCM (R403Q, R453C) and two DCM (S532P, F764L) mutant myosins isolated from homozygous mouse models using a novel load-clamped laser trap assay. F_{max} was 50% (R403Q) and 80% (R453C) greater for the HCM mutants compared with the wild type, whereas F_{max} was severely depressed for one of the DCM mutants (65% S532P). Although F_{max} was normal for the F764L DCM mutant, its actin-activated ATPase activity and actin filament velocity (V_{actin}) in a motility assay were significantly reduced (Schmitt JP, Debold EP, Ahmad F, Armstrong A, Frederico A, Conner DA, Mende U, Lohse MJ, Warshaw D, Seidman CE, Seidman JG. *Proc Natl Acad Sci USA* 103: 14525–14530, 2006.). These F_{max} data combined with previous V_{actin} measurements suggest that HCM and DCM result from alterations to one or more of myosin's fundamental mechanical properties, with HCM-causing mutations leading to enhanced but DCM-causing mutations leading to depressed function. These mutation-specific changes in mechanical properties must initiate distinct signaling cascades that ultimately lead to the disparate phenotypic responses observed in HCM and DCM.

familial hypertrophic cardiomyopathy; in vitro motility; force-velocity relationship; heart failure

INHERITED CARDIOMYOPATHIES resulting from point mutations in sarcomeric proteins can produce distinctly different clinical phenotypes (46). Hypertrophic cardiomyopathy (HCM) is characterized by enlarged ventricular walls, fibrosis, and myocyte disarray (46). Despite these morphological changes, cardiac function is maintained or even enhanced (22). In contrast, patients with inheritable dilated cardiomyopathy (DCM) display decompensated cardiac hypertrophy with distended, thinly walled ventricles and decreased contractility (1, 35, 44, 46). Because mutations in myosin, the heart's molecular motor, are linked to both HCM and DCM (46), characterizing the effects of these mutations on myosin's force and motion generation provides a unique opportunity to understand *1*) how functional alterations lead to such divergent clinical phenotypes and *2*) how myosin's structure determines its molecular mechanics.

Myosin mechanical performance, associated with HCM-causing mutations, has been characterized using human striated muscle biopsies (2, 4, 5, 30, 33), murine models (38, 48), and protein expression systems (42, 55). Decreased motion generation was initially observed for various HCM-myosin mutants both in human fiber studies and in an in vitro motility assay, which serves as a molecular model system for unloaded shortening velocity. Maximal isometric force was also reduced in skinned soleus fibers that express HCM mutant myosin (30, 33) and in expressed *Dictyostelium* myosin possessing HCM-causing mutations as characterized in a laser trap assay (10). Thus HCM myosin mutations may lead to a compromised motor. However, enhanced motion and force generation were observed in the motility assay for mutant myosin from human and murine cardiac tissue as well as mutations expressed in heterologous myosin backbones (2, 29, 38, 39, 48, 55). Therefore the effect of HCM mutations on myosin mechanical performance remains equivocal.

Cardiac myosin point mutations and mutations in other sarcomeric proteins have been linked to DCM (7, 15, 27, 28, 31, 34, 36, 37, 44, 45, 49). Using murine models homozygous for mutations in either the actin-binding (S532P) or converter domain (F764L), we observed significant reductions in both actin-activated myosin ATPase activity and actin filament velocity (V_{actin}) for these mutants compared with wild-type (WT) cardiac myosin without any effect on maximal average force production (43). Our previous studies suggested that enhanced function may be characteristic of HCM myosin mutants, and the reduced hydrolytic and motion-generating capacity for the DCM mutants implies that the manner in which myosin's molecular mechanics are altered may be a primary determinant of the clinical phenotype.

In the past, we have used the in vitro motility assay to characterize both myosin's unloaded velocity and maximum force production. However, force production was determined indirectly using a model-dependent mixtures assay, which assumes a molecular tug-of-war between myosins having sub-

Address for reprint requests and other correspondence: D. M. Warshaw, Univ. of Vermont, Dept. of Molecular Physiology and Biophysics, College of Medicine, 149 Beaumont Ave., HSRF Bldg., Rm. 116, Burlington, VT 05405 (e-mail: warshaw@physiology.med.uvm.edu).

The costs of publication of this article were defrayed in part by the payment of page charges. The article must therefore be hereby marked "*advertisement*" in accordance with 18 U.S.C. Section 1734 solely to indicate this fact.

stantially different V_{actin} (19). The mixture assay suffers in that the absolute force production cannot be obtained and is insensitive when relative force differences between myosins become large. However, a direct measure of myosin's average maximum isometric force generation is now possible from a small myosin ensemble (<20 molecules) using the laser trap force clamp assay (8). With this new method, we characterized and compared the force-generating capacity of two HCM (R403Q, R453C) and two DCM (S532P, F764L) mutants isolated from homozygous murine models. The R453C, characterized for the first time, and the other R403Q HCM mutant generated significantly higher forces than WT, whereas one of the DCM mutants (S532P) produced only one-third the force of WT. Although the force generation was normal for the F764L DCM mutant, its actin-activated ATPase activity and V_{actin} in a motility assay were significantly reduced (43). These differences in force and in V_{actin} suggest that alterations to one or more of myosin's mechanical properties is sufficient to initiate a differential genetic program so that enhanced function leads to the HCM phenotype, whereas depressed function is characteristic of DCM.

METHODS

Proteins. Two HCM-causing mutations, one in myosin's actin-binding domain (R403Q; see Ref. 41) and another near the ATP-binding site (R453C), and two DCM-causing mutations, one in the lower 50-kDa region of the actin-binding domain (S532P) and another in the converter region (F764L), were engineered into the mouse α-myosin heavy chain as previously described (12, 43). Mice homozygous for the HCM-causing mutations died within ~7 days of birth; therefore, hearts (~20 mg) were harvested from ~7-day-old pups (9). In contrast, mice possessing DCM-causing mutations rapidly developed symptoms of DCM but lived to adulthood (43) so that left ventricles were harvested between 10 and 30 wk old, providing an ~40-mg sample for isolation as was the case for WT cardiac myosin. All protocols compiled with the *Guide for the Use and Care of Laboratory Animals* published by the National Institutes of Health. All of the mice were treated in accordance with the guidelines of the Animal Care and Use Committee of Harvard University.

Cardiac myosin was isolated using methods previously employed by our laboratory for samples as small as 10 mg (48). Briefly, heart tissue was homogenized for 20 min in a high-salt buffer [1:5 wt/vol (in M), 0.3 KCl, 0.15 K_2HPO_4, 0.01 Na_4PO_7, 0.001 $MgCl_2$, and 0.002 dithiothreitol (DTT), pH 6.8] followed by ultracentrifugation for 1 h at 150,000 *g*. Filamentous myosin was precipitated from the supernatant and pelleted by ultracentrifugation for 20 min at 50,000 *g* and resuspended in myosin buffer (in M: 0.025 imidazole, 0.004 $MgCl_2$, 0.01 DTT, 0.001 EGTA, and 0.3 KCl, at pH 7.4). Before each experiment, the isolated myosin was ultracentrifuged at 95,000 *g* in the presence of actin and ATP to remove inactive myosin molecules from the preparation. Following this procedure, the myosin concentration was determined by a Bradford (3) assay using commercially available reagents from Bio-Rad Laboratories.

In vitro motility assay. The ability of mutant myosin to translocate actin was assessed in the in vitro motility assay (53) as previously described (17, 54). Briefly, isolated myosin was adhered to a nitrocellulose-coated cover slip surface at either 15 or 100 μg/ml, and the velocity of fluorescently-labeled actin filaments was determined at an ATP concentration of either 100 μM or 1 mM ATP. The results from two to five separate mouse heart preparations were averaged to yield the mean V_{actin}.

Load-clamp laser trap assay. A three-bead laser trap assay (16, 26) was modified to incorporate a feedback circuit enabling the application of constant loads to an actin filament sliding across a myosin-coated surface (Fig. 1) as previously described (8). This was accomplished by taking advantage of the spring-like nature of the optical trap as described by Visscher et al. (50). Specifically, the laser position was controlled through an acousto-optic deflector (AOD; NEOS technologies) with a rise/fall time of <100 ns using custom software running on a real-time Linux operating system with dual Pentium 4 processors. The actin filament position was monitored with nanometer resolution by detecting the bead attached to the filament's end on a quadrant-photodiode detector.

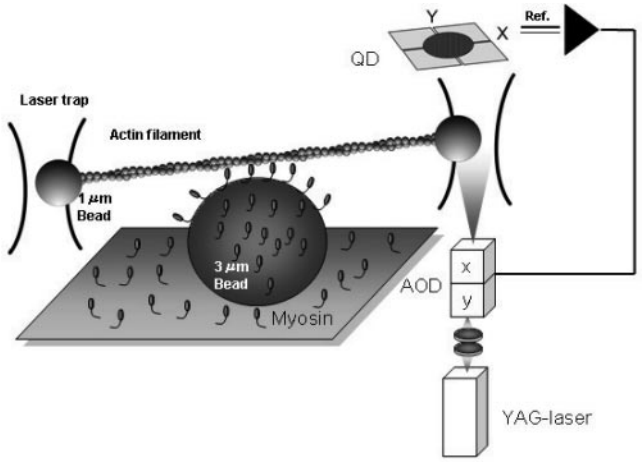

Fig. 1. Schematic representation of the load-clamp laser trap assay in which the standard 3-bead assay (26) was modified to allow a single actin filament to interact with a miniensemble of cardiac myosin molecules under a constant load. An actin filament was attached to two 1-μm beads and brought in contact with a 3-μm diameter bead on a cover slip surface coated with myosin at a concentration such that ~4 molecules were available to interact with the actin filament (see text). The load-clamp was achieved by detecting the actin filament position (i.e., bead position) using the quadrant photodiode (QD) to determine the distance the bead is from trap center (i.e., load). To maintain a constant load, the position of the laser beam was controlled by an acousto-optic deflector (AOD) so that the distance between the bead and trap center was maintained constant.

When the actin filament contacted the myosin-coated surface on a 3-μm diameter silica bead, the bead-actin-bead assembly was pulled away from the trap center by the myosin until the desired load was achieved (a value equal to the displacement from trap center times the trap stiffness). At this point, the trap center was moved by the AOD to maintain a fixed distance from the bead, i.e., constant force. Loads (1–8 pN) were applied to the actin filament with step durations ranging from 80 to 200 ms in ascending and then descending order in 1-pN increments. The order of the applied load did not affect the velocity measurements (data not shown).

Cardiac myosin was adhered to a nitrocellulose cover slip, as described above for the motility assay, at concentrations of 15 μg/ml, except for S532P DCM mutant, which required 60 μg/ml to record load-clamp responses.

Force-velocity relationships. Force-velocity (F-*V*) relationships (Fig. 2) were generated from the load-clamp data as follows. Displacement traces during each load-clamp step were fitted to least-squares regression lines, the slopes of which equaled the velocity at that load. For a given actin filament and heart preparation, multiple velocities (10–120) were obtained at each load and then averaged across heart preparations (2–5). The velocity at zero load was obtained separately by measuring V_{actin} in the motility assay (53) under identical assay conditions as those in the laser trap. The velocity vs. load data were fit to the Hill F-*V* equation: $(F + a)(V + b) = (F_{max} + a)b$, where F is force, *V* is velocity, and *a* and *b* are constants in units of force and velocity, respectively (21).

Although F-*V* relationships characterize a myosin's performance under load, we have used the F-*V* relation only to estimate myosin's

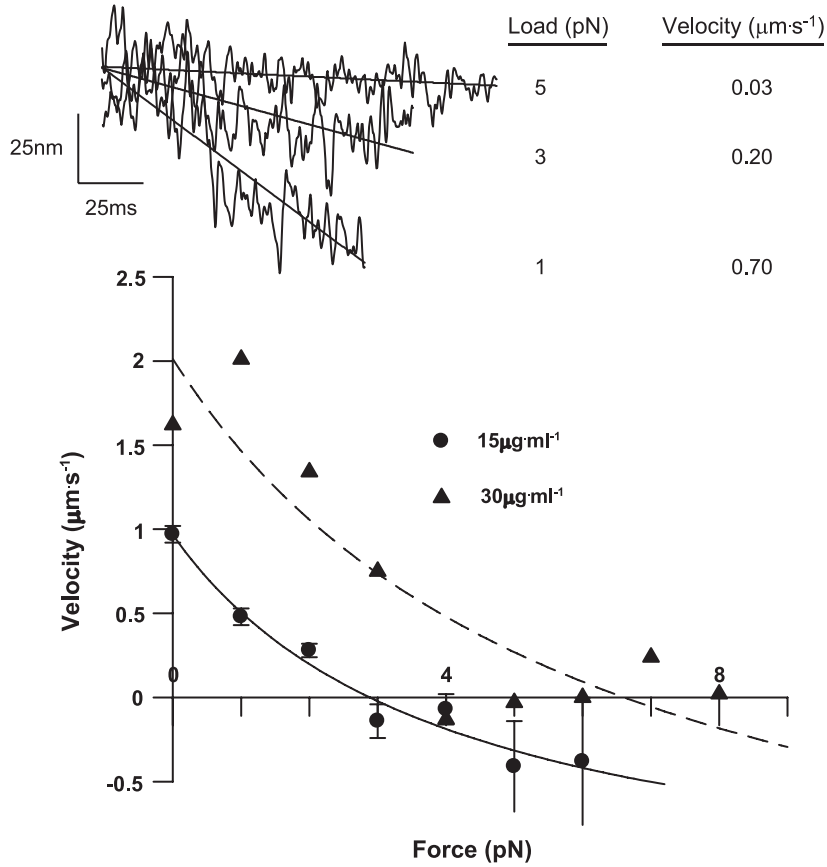

Fig. 2. Wild-type (WT) force vs. velocity relations for myosin concentrations of 15 (circles) and 30 (triangles) μg/ml. Sample actin filament displacement traces (filtered at 200 Hz) at various loads are presented with their corresponding velocities determined by the slope of the linear regression. The 0 load velocity was obtained by actin filament velocity (V_{actin}) in the motility assay under the same conditions as in the laser trap assay (see text). The loaded actin filament velocities are the average (±SE) of 10–100 values at each load with the relationship fit with the Hill force-velocity equation (see text and Table 2 for parameters of the fit).

maximum isometric force generation (F_{max}). F_{max} was derived from an interpolation of the best-fit F-*V* relation at isometric conditions (i.e., 0 velocity). We elected not to draw any other inferences about myosin function based on changes in the shape of the F-*V* relationship for the following reasons. F_{max} is a straightforward mechanical index that is directly proportional to the number of attached myosin heads, as observed when increasing the myosin concentration twofold from 15 to 30 μg/ml (Fig. 2). To keep F_{max} and the applied loads in the useable range of the force clamp assay (1–8 pN), myosin concentrations (≤30 μg/ml) resulting in subsaturating surface conditions were used. Under these conditions, V_{actin} in the motility assay is a nonlinear function of the number of myosin heads that interact with the actin filament (18) such that differences in V_{actin} that exist under saturating conditions (≥100 μg/ml) may not exist at subsaturating conditions (see Fig. 4). As a result, interpretive comparisons based on the shape of the F-*V* relationships is extremely difficult. However, the F-*V* relationship can still be used as a determinant of F_{max}.

Myosin surface density measurements. With F_{max} proportional to the number of myosin heads attached to the actin filament, myosin head density on the nitrocellulose-coated cover slip surface is required to normalize F_{max} on a per head basis across the various mutants. The myosin surface density at a given myosin concentration (15 or 100 μg/ml) infused in the experimental flowcell was estimated by comparing the rate of NH_4- and EDTA-dependent P_i release by WT α-cardiac myosin on the motility surface with a standard curve measured for known myosin concentrations in solution (Fig. 3*A*), as previously described (18). This determines the total number of hydrolytically competent heads on the surface and, when divided by the cover slip surface dimensions, provides an estimate of the myosin head density per square micrometer. If we assume, based on myosin's structural dimensions, that myosin heads within 26 nm of the actin filament center can interact with the actin filament (18), then 15 ± 3 and 48 ± 7 heads are available to interact per micrometer of actin filament length at myosin concentrations of 15 and 100 μg/ml, respectively (Fig. 3*B*). With these estimates being similar to our previous estimates for both skeletal and smooth muscle myosin on a comparable surface (18), it appears that whole muscle myosin, regardless of the isoform, adheres similarly to the cover slip surface. This is not surprising, since the mode of attachment is believed to be through the myosin tail region (47). Thus we assume that the surface densities are similar for all myosins studied since none of the mutations is in the myosin tail.

Finally, knowing the geometry of the physical setup in the load-clamp assay, it is possible to estimate that only a 0.5-μm length of actin filament can interact with the myosin-coated surface in the laser trap. At the 15 μg/ml myosin concentrations, we estimate that, on average, eight myosin heads (i.e., 4 molecules) are available to interact with the actin filament.

RESULTS

V_{actin}. The unloaded V_{actin} in the motility assay under saturating myosin surface conditions and 1 mM ATP revealed that the R403Q HCM mutant translocated actin 24% faster than WT, although the R453C HCM mutant was unchanged (Table 1). These values are in contrast to our previously measured V_{actin} for the S532P and F764L DCM mutants, which both demonstrated a significant decrease in V_{actin} compared with WT (data taken from Ref. 43).

F_{max}. To determine F_{max} for the various mutants, F-*V* relationships were obtained for each mutant and compared with WT (Fig. 4). As previously described for skeletal muscle myosin (8), cardiac myosin generated actin filament velocities that declined in a hyperbolic fashion with increasing load. This relationship, over the entire range of loads, was well fit

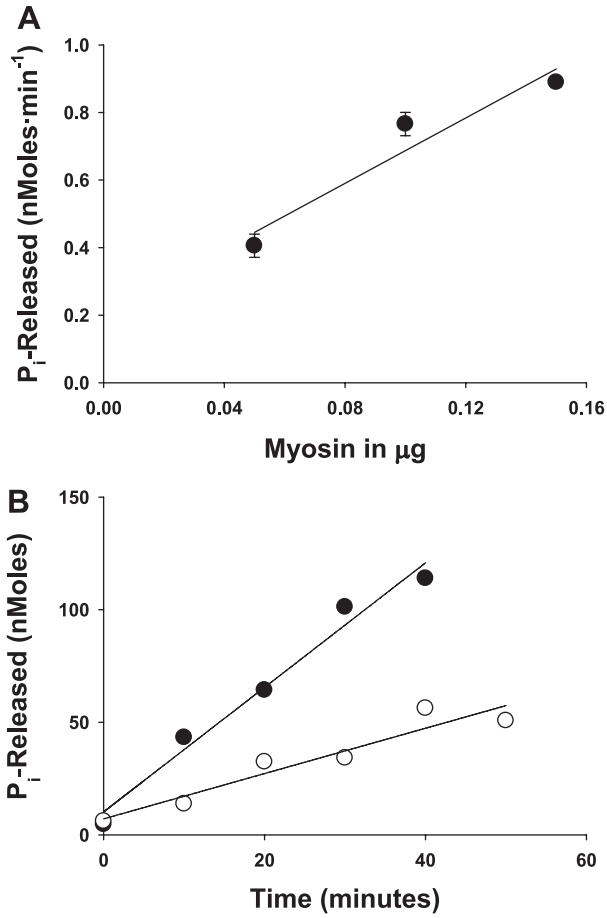

Fig. 3. Quantification of the number of myosin heads on the motility surface available to interact per μm of actin using WT myosin. The rate of P_i release was initially determined in solution as a function of increasing amounts of myosin (*A*, symbols represent means ± SE). The amount of P_i released at surface densities of 15 (open symbols) and 100 (filled symbols) μg/ml was determined at 10-min intervals (*B*) using a colorimetric assay (see METHODS). The slopes of the lines (i.e., ATPase rate) were used to estimate the no. of heads available to interact with actin as described in the text.

(R^2 value >0.95) by the Hill F-*V* equation (21; Figs. 2 and 4; see Table 2 for fit parameters). Because it was impossible to know in advance what load would be required to stall the actin filament, we empirically chose a range of loads that would go beyond isometric conditions to better help define F_{max}. Thus the *x*-intercept for the F-*V* fit was taken as F_{max}. For WT myosin using 15 μg/ml myosin, an F_{max} of 2.89 ± 0.28 pN was generated by eight myosin heads (see above) so that each WT head generated 0.36 ± 0.04 pN.

F_{max}/head were then obtained for the DCM and HCM mutants, and the results are shown in Fig. 4 and Table 2. For each myosin, the 95% confidence intervals were constructed around the predicted F_{max} and used to determine differences between mutant and WT myosins.

The S532P DCM mutant, which was characterized by a significantly slower V_{actin}, had such a low force-generating capacity that it required a fourfold greater myosin concentration (60 μg/ml) to produce sufficient force to allow the load-clamp assay to operate in its desirable range of loads (see above). This was not because of poor surface binding of S532P myosin, since the estimated surface density, based on surface ATPase measurements, was similar to that of WT (data not shown). Given the estimated F_{max}, it appears that the S532P DCM mutant can only generate one-third the F_{max} of WT (Table 2), whereas the F764L DCM mutant, which had a diminished V_{actin}, was capable of generating comparable F_{max} to WT (Fig. 4, Table 2).

In contrast, both the R403Q and R453C HCM mutants generated 50 and 83% greater F_{max} than WT (Fig. 4 and Table 2). The enhanced F_{max} for the R403Q confirms an earlier study using the motility mixtures assay that predicted enhanced F_{max} (48).

DISCUSSION

With point mutations in the cardiac myosin motor domain responsible for two distinct cardiomyopathies, we investigated whether alterations to myosin's molecular mechanics would be predictive of the clinical outcome. We took advantage of mouse models that produce different mutant α-cardiac myosins. Two of these mutant proteins lead to HCM (R403Q, R453C; see Refs. 12 and 38) and two lead to DCM (S532P, F764L; see Ref. 43). The myosin, purified from these animals, was then characterized using the load-clamp laser trap assay to determine their force-generating capacity. These measurements represent the first direct estimates of force generation for these mutant myosins at the molecular level, eliminating the uncertainties of previous estimates using an indirect, model-dependent mixtures motility assay (19).

For each mutant myosin, we measured V_{actin} and F_{max}; however, actin-activated myosin ATPase activities were determined previously (43, 48). These mechanical and enzymatic data are summarized in Fig. 5. Compared with WT, it appears that one or more functional indexes are enhanced for the HCM mutants, whereas the opposite is true for the DCM mutants, as discussed below.

HCM and DCM mutant myosin molecular mechanics. The R403Q mutation is the most extensively characterized, being the first contractile protein mutation linked to HCM (13). This mutation enhances the mechanical and hydrolytic properties of mouse α-cardiac myosin and other myosin isoforms into which the mutation was introduced (29, 39, 48, 52, 55). These findings are in contrast to other studies reporting depressed V_{actin} (5, 6, 42) and force generation in either *Dictyostelium*

Table 1. *V_{actin} at a myosin surface concentration of 100 μg/ml and at 1 mM ATP*

	WT	S532P	*P*	F764L	*P*	R403Q	*P*	R453C	*P*
V_{actin}, μm/s	4.2 (SD0.7)*	2.4 (SD0.3)*	<0.05	3.4 (SD0.4)*	<0.05	5.2 (SD0.7)	<0.05	4.0 (SD0.9)	NS
n	20	18		6		3		2	

Actin filament velocities (V_{actin}) are means with SD in parentheses; *n*, no. of mouse heart preparations used to determine means and SDs. WT, wild type. Differences were quantified using a one-way ANOVA with a Student-Newman-Keuls post hoc test used to locate significant differences at $P < 0.05$ vs. WT. *Data reprinted from Schmitt et al. (43) for comparative purposes. NS, not significant.

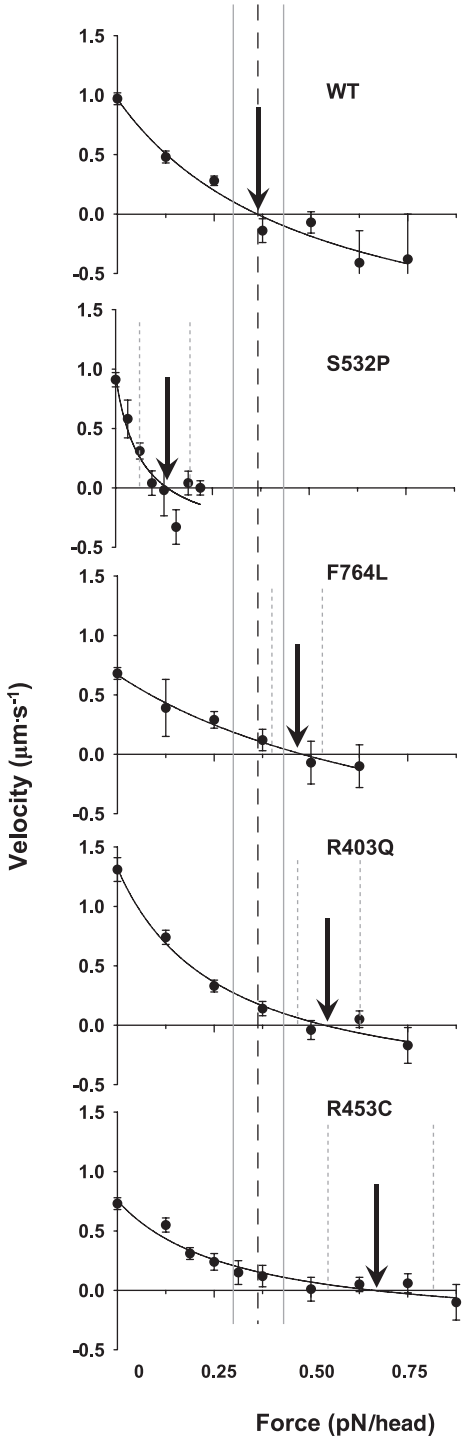

Fig. 4. Force-velocity relationships for WT and mutant myosins. Each curve is the combined results from at least 2 hearts/mutant, with each point representing the mean of 10–120 velocities and error bars indicating ±SE. The curves were fitted by least squares to the Hill force-velocity equation as in Fig. 2. The S532P mutant force data are corrected for increased myosin concentration required compared with WT. The solid arrow indicates F_{max} for each myosin. The gray lines indicate the ±95% confidence intervals around WT F_{max}, whereas the dotted lines represent the ±95% confidence intervals for the mutant F_{max}.

myosin (10) or human skeletal muscle fibers (30). The reason for the discrepancy remains unclear but is the subject of a detailed review that offers possible explanations related to differences in protein expression systems and isolation procedures for myosin (32). Additionally, the absence of muscle regulatory proteins in the present set of experiments may also help to explain this discrepancy, since isolated muscle preparations (30, 33) typically contain a full compliment of troponin and tropomyosin, which are known to modulate the kinetics of the actomyosin interaction (24).

F_{max} for the R453C HCM mutant was the only altered functional property, but its enhancement was far greater than the R403Q (see Fig. 5). However, in mice heterozygous for the mutation, maximal isometric force was not altered in cardiac muscle strips (38). The enhanced force production reported here for the R453C mutant may result from compounding or cooperative effects, since both myosin heads have the mutation. In addition, the motility-based studies reported here use unregulated actin, eliminating any potential modulation that actin regulatory proteins may impart in vivo (23).

For the DCM mutants, mechanical performance was depressed, with both the S532P and F764L substitutions reducing V_{actin} while F_{max} was severely depressed for the S532P (see Fig. 5).

At the molecular level, F_{max} per head is the product of myosin's unitary force (F_{uni}) generated by the power stroke and its duty ratio (f, defined as the fraction of the ATPase cycle spent strongly bound to actin; see Ref. 16):

$$F_{max} = F_{uni} \times f$$

Therefore, the alterations in F_{max} for the HCM and DCM mutants could be attributed to changes in either myosin's inherent mechanical (F_{uni}) and/or kinetic (f) properties. F_{uni} can only be measured at the single molecule level, and for the R403Q mutant we have previously shown that F_{uni} is the same as WT (48), suggesting that at least for the R403Q mutant an alteration to one or more steps in the cross-bridge cycle most likely occurred such that the duty ratio is increased under load. Which step is altered is a matter of speculation, but with the release of ADP from the myosin active site being sensitive to load and rate limiting for detachment from the strongly bound state, this step would be a candidate for investigation (25). In contrast, we have previously shown that, in the laser trap under unloaded conditions, both the unitary displacement (d) and strongly bound time (t_{on}) are altered in the S532P DCM mutant, which fully accounted for the depressed V_{actin} for this mutant (43). These changes do suggest that, under unloaded conditions, both the inherent mechanical and kinetic properties can be affected by a single point mutation.

Myosin mutant structural considerations. Do the mutant's structural locations within the myosin motor domain offer insight to the origin of their effects? The R403Q HCM and S532P DCM mutants exist within the actin-binding interface, which is split by a cleft that separates the upper and lower 50-kDa segments. The opening and closure of this cleft are linked to both the kinetics of ATP hydrolysis at the active site and long-range communication between the actin-binding domain and rotation of the myosin lever arm via the active site (11). With the dynamics of cleft movement so crucial to myosin's mechanics and kinetics, it is not surprising that both the R403Q and S532P mutants have such significant effects, since they reside on opposite sides of the cleft. Specifically, the R403Q mutation resides in the upper 50-kDa segment near a surface loop that forms the initial weak electrostatic interaction between actin and myosin, whereas the S532P lies in a highly

Table 2. *Summary of maximal isometric force values and Hill force-velocity parameters*

	WT	S532P	*P*	F764L	*P*	R403Q	*P*	R453C	*P*
F_{max}, pN/head	0.36±0.04	0.13±0.04*	<0.05	0.48±0.04	NS	0.54±0.05*	<0.05	0.66±0.09*	<0.05
a, pN	4.0±2.0	0.5±0.4		7.0±4.1		2.1±0.6		2.4±0.9	
b, μm/s	1.3±0.5	0.5±0.3		0.5±0.4		0.7±0.2		0.4±0.1	

Values represent means ± SE. Maximal force-generating capacity (F_{max}) values were subjected to a one-way ANOVA and a Newman-Keuls post hoc test when appropriate, WT vs. mutant. *a* and *b,* Constants of the fit for the Hill force-velocity equation.

conserved α-helix in the lower 50-kDa segment that forms the strong, hydrophobic actomyosin interaction (40). Why these mutations have such opposing effects on myosin mechanics is intriguing. However, choosing the S532P as an example, it is possible that the proline substitution at residue 532 breaks the helix in which it resides, preventing proper formation of the strong, stereospecific bond between actin and myosin. This may disrupt closure of the cleft, preventing proper lever arm rotation (51) and thus accounting for the severely decreased force and motion generation as well as alterations to the kinetics of ATP hydrolysis (43).

The R453C HCM mutation is near the ATP-binding site. The observed increase in F_{max} may be due to the removal of a positive charge, altering the nucleotide-binding affinity so that a slowed rate of ADP release might increase the duty ratio. In support of this, an increased duty ratio was observed when the mutation was introduced into skeletal muscle myosin (52). The F764L DCM mutant is located in the converter region that transmits conformational changes in the active site to the myosin lever arm. With the converter domain critical to intramolecular communication within the myosin molecule and with the motor so sensitive to load, it is apparent that even a conservative substitution of one hydrophobic (Phe) residue for another (Leu) is sufficient to alter myosin's mechanical and hydrolytic performance. Interestingly, despite a reduction in V_{actin} and the maximal ATPase rate, F_{max} was similar to that of WT for F764L, suggesting that the development of the phenotype is not initiated through the sensation of maximal force for this mutation.

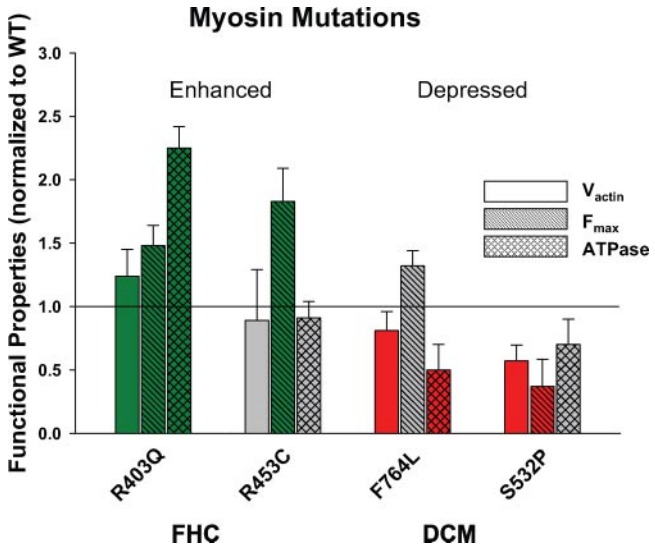

Fig. 5. Comparison of V_{actin}, F_{max}, and actin-activated ATPase values for HCM- and DCM-causing mutations relative to WT as indicated by the horizontal line. Green, significant increase; red, significant decrease; gray, statistically similar to WT. Values displayed are means ± SE. All data are from the present study; however, V_{actin} and ATPase data for S532P and F764L are reprinted from Schmitt et al. (43) and the R403Q ATPase data are reprinted from Tyska et al. (48).

Functional alterations are predictive of clinical phenotype. Figure 5 summarizes the alterations to myosin's mechanical and hydrolytic properties for the HCM and DCM mutants studied here. These results suggest that compromised myosin function is not a common theme for all inherited cardiomyopathies but that the HCM and DCM mutations lead to differential effects. Specifically, HCM-causing mutations enhance one or more molecular indexes of myosin function with the opposite effect brought about by the DCM-causing mutations and; these primary insults to myosin performance may dictate the specific clinical phenotype. In addition, the enhanced V_{actin} and F_{max} for the R403Q mutation may offer a potential molecular explanation for the increased contractility observed in whole heart studies both in the mouse model (14) and in humans (22). It is worth noting that mice homozygous for the DCM-causing mutations live to adulthood (43) despite having depressed molecular motor function, whereas mice homozygous for either HCM-causing mutation die within days after birth (9). Thus DCM mice can compensate for a compromised motor and mimic the disease progression in humans, with symptoms developing slowly in DCM patients while sudden death is common for the HCM mutations studied (46).

From this limited data set, it appears that the primary insult to at least one of myosin's molecular properties (see Fig. 5) is sufficient to trigger the cascade of events that leads to disease and that this insult can be to V_{actin}, F_{max}, or both. Although it seems improbable that all of the many mutations in sarcomeric proteins linked to cardiomyopathies (46) will follow the same pattern, two additional HCM-causing mutations in the rod portion of myosin (2, 39) also demonstrated enhanced V_{actin}, and DCM-causing mutations in the muscle regulatory proteins troponin and tropomyosin decrease several myofibrillar parameters, including V_{actin} (35). Thus the finding of enhanced function in HCM and decreased function in DCM-causing mutations appears to extend beyond the four mutations examined in the present study. Parallel signaling pathways do exist within the myocyte (20) that are sensitive to myocyte mechanics, making it possible that these pathways are specific to sensing changes in motion (V_{actin}) vs. force generation (F_{max}). If so, future therapies might target a specific pathway once knowing how a mutation in myosin or any other sarcomeric protein alters the force and motion-generating capacity of the sarcomere.

ACKNOWLEDGMENTS

We thank A. Armstrong and A. Federico for performing ATPase measurements; N. Kad, J. Baker, and Y. Ali for thoughtful discussions during the

collection and analysis of these data; and Guy Kennedy for support of the mechanooptical instrumentation.

GRANTS

This work was supported by the Henrietta and Frederick Bugher Fund (J. G. Seidman), the Howard Hughes Medical Institute (C. Seidman), the National Institutes of Health (D. M. Warshaw, C. Seidman, and J. G. Seidman), and the Deutsche Stiftung für Herzforschung (J. P. Schmitt).

REFERENCES

1. **Ahmad F, Seidman JG, Seidman CE.** The genetic basis for cardiac remodeling. *Annu Rev Genomics Hum Genet* 6: 185–216, 2005.
2. **Alpert NR, Mohiddin SA, Tripodi D, Jacobson-Hatzell J, Vaughn-Whitley K, Brosseau C, Warshaw DM, Fananapazir L.** Molecular and phenotypic effects of heterozygous, homozygous, and compound heterozygote myosin heavy-chain mutations. *Am J Physiol Heart Circ Physiol* 288: H1097–H1102, 2005.
3. **Bradford MM.** A rapid and sensitive method for the quantitation of microgram quantities of protein utilizing the principle of protein-dye binding. *Anal Biochem* 72: 248–254, 1976.
4. **Cuda G, Fananapazir L, Epstein ND, Sellers JR.** The in vitro motility activity of beta-cardiac myosin depends on the nature of the beta-myosin heavy chain gene mutation in hypertrophic cardiomyopathy. *J Muscle Res Cell Motil* 18: 275–283, 1997.
5. **Cuda G, Fananapazir L, Zhu WS, Sellers JR, Epstein ND.** Skeletal muscle expression and abnormal function of beta-myosin in hypertrophic cardiomyopathy. *J Clin Invest* 91: 2861–2865, 1993.
6. **Cuda G, Pate E, Cooke R, Sellers JR.** In vitro actin filament sliding velocities produced by mixtures of different types of myosin. *Biophys J* 72: 1767–1779, 1997.
7. **Daehmlow S, Erdmann J, Knueppel T, Gille C, Froemmel C, Hummel M, Hetzer R, Regitz-Zagrosek V.** Novel mutations in sarcomeric protein genes in dilated cardiomyopathy. *Biochem Biophys Res Commun* 298: 116–120, 2002.
8. **Debold EP, Patlak JB, Warshaw DM.** Slip sliding away: load-dependence of velocity generated by skeletal muscle Myosin molecules in the laser trap. *Biophys J* 89: L34–L36, 2005.
9. **Fatkin D, Christe ME, Aristizabal O, McConnell BK, Srinivasan S, Schoen FJ, Seidman CE, Turnbull DH, Seidman JG.** Neonatal cardiomyopathy in mice homozygous for the Arg403Gln mutation in the alpha cardiac myosin heavy chain gene. *J Clin Invest* 103: 147–153, 1999.
10. **Fujita H, Sugiura S, Momomura S, Omata M, Sugi H, Sutoh K.** Characterization of mutant myosins of Dictyostelium discoideum equivalent to human familial hypertrophic cardiomyopathy mutants. Molecular force level of mutant myosins may have a prognostic implication. *J Clin Invest* 99: 1010–1015, 1997.
11. **Geeves MA, Holmes KC.** Structural mechanism of muscle contraction. *Annu Rev Biochem* 68: 687–728, 1999.
12. **Geisterfer-Lowrance AA, Christe M, Conner DA, Ingwall JS, Schoen FJ, Seidman CE, Seidman JG.** A mouse model of familial hypertrophic cardiomyopathy. *Science* 272: 731–734, 1996.
13. **Geisterfer-Lowrance AA, Kass S, Tanigawa G, Vosberg HP, McKenna W, Seidman CE, Seidman JG.** A molecular basis for familial hypertrophic cardiomyopathy: a beta cardiac myosin heavy chain gene missense mutation. *Cell* 62: 999–1006, 1990.
14. **Georgakopoulos D, Christe ME, Giewat M, Seidman CM, Seidman JG, Kass DA.** The pathogenesis of familial hypertrophic cardiomyopathy: early and evolving effects from an alpha-cardiac myosin heavy chain missense mutation. *Nat Med* 5: 327–330, 1999.
15. **Gerull B, Atherton J, Geupel A, Sasse-Klaassen S, Heuser A, Frenneaux M, McNabb M, Granzier H, Labeit S, Thierfelder L.** Identification of a novel frameshift mutation in the giant muscle filament titin in a large Australian family with dilated cardiomyopathy. *J Mol Med* 84: 478–483, 2006.
16. **Guilford WH, Dupuis DE, Kennedy G, Wu J, Patlak JB, Warshaw DM.** Smooth muscle and skeletal muscle myosins produce similar unitary forces and displacements in the laser trap. *Biophys J* 72: 1006–1021, 1997.
17. **Harris DE, Warshaw DM.** Smooth and skeletal muscle actin are mechanically indistinguishable in the in vitro motility assay. *Circ Res* 72: 219–224, 1993.
18. **Harris DE, Warshaw DM.** Smooth and skeletal muscle myosin both exhibit low duty cycles at zero load in vitro. *J Biol Chem* 268: 14764–14768, 1993.
19. **Harris DE, Work SS, Wright RK, Alpert NR, Warshaw DM.** Smooth, cardiac and skeletal muscle myosin force and motion generation assessed by cross-bridge mechanical interactions in vitro. *J Muscle Res Cell Motil* 15: 11–19, 1994.
20. **Heineke J, Molkentin JD.** Regulation of cardiac hypertrophy by intracellular signalling pathways. *Nat Rev Mol Cell Biol* 7: 589–600, 2006.
21. **Hill AV.** The heat of shortening and the dynamic constants of muscle. *Proc R Soc Lond B Biol Sci* 126: 136–195, 1938.
22. **Ho CY, Sweitzer NK, McDonough B, Maron BJ, Casey SA, Seidman JG, Seidman CE, Solomon SD.** Assessment of diastolic function with Doppler tissue imaging to predict genotype in preclinical hypertrophic cardiomyopathy. *Circulation* 105: 2992–2997, 2002.
23. **Homsher E, Lee DM, Morris C, Pavlov D, Tobacman LS.** Regulation of force and unloaded sliding speed in single thin filaments: effects of regulatory proteins and calcium. *J Physiol* 524: 233–243, 2000.
24. **Homsher E, Nili M, Chen IY, Tobacman LS.** Regulatory proteins alter nucleotide binding to acto-myosin of sliding filaments in motility assays. *Biophys J* 85: 1046–1052, 2003.
25. **Kad NM, Patlak JB, Fagnant PM, Trybus KM, Warshaw DM.** Mutation of a conserved glycine in the SH1-SH2 helix affects the load-dependent kinetics of myosin. *Biophys J* 92: 1623–1631, 2007.
26. **Kad NM, Rovner AS, Fagnant PM, Joel PB, Kennedy GG, Patlak JB, Warshaw DM, Trybus KM.** A mutant heterodimeric myosin with one inactive head generates maximal displacement. *J Cell Biol* 162: 481–488, 2003.
27. **Kamisago M, Sharma SD, DePalma SR, Solomon S, Sharma P, McDonough B, Smoot L, Mullen MP, Woolf PK, Wigle ED, Seidman JG, Seidman CE.** Mutations in sarcomere protein genes as a cause of dilated cardiomyopathy. *N Engl J Med* 343: 1688–1696, 2000.
28. **Karkkainen S, Miettinen R, Tuomainen P, Karkkainen P, Helio T, Reissell E, Kaartinen M, Toivonen L, Nieminen MS, Kuusisto J, Laakso M, Peuhkurinen K.** A novel mutation, Arg71Thr, in the delta-sarcoglycan gene is associated with dilated cardiomyopathy. *J Mol Med* 81: 795–800, 2003.
29. **Keller DI, Coirault C, Rau T, Cheav T, Weyand M, Amann K, Lecarpentier Y, Richard P, Eschenhagen T, Carrier L.** Human homozygous R403W mutant cardiac myosin presents disproportionate enhancement of mechanical and enzymatic properties. *J Mol Cell Cardiol* 36: 355–362, 2004.
30. **Lankford EB, Epstein ND, Fananapazir L, Sweeney HL.** Abnormal contractile properties of muscle fibers expressing beta-myosin heavy chain gene mutations in patients with hypertrophic cardiomyopathy. *J Clin Invest* 95: 1409–1414, 1995.
31. **Li D, Czernuszewicz GZ, Gonzalez O, Tapscott T, Karibe A, Durand JB, Brugada R, Hill R, Gregoritch JM, Anderson JL, Quinones M, Bachinski LL, Roberts R.** Novel cardiac troponin T mutation as a cause of familial dilated cardiomyopathy. *Circulation* 104: 2188–2193, 2001.
32. **Lowey S.** Functional consequences of mutations in the myosin heavy chain at sites implicated in familial hypertrophic cardiomyopathy. *Trends Cardiovasc Med* 12: 348–354, 2002.
33. **Malinchik S, Cuda G, Podolsky RJ, Horowits R.** Isometric tension and mutant myosin heavy chain content in single skeletal myofibers from hypertrophic cardiomyopathy patients. *J Mol Cell Cardiol* 29: 667–676, 1997.
34. **Martins E, Silva-Cardoso J, Alves C, Pereira H, Soares B, Damasceno A, Abreu-Lima C, Amorim A, Rocha-Goncalves F.** Familial dilated cardiomyopathy with troponin T K210del mutation. *Rev Port Cardiol* 25: 295–300, 2006.
35. **Mirza M, Marston S, Willott R, Ashley C, Mogensen J, McKenna W, Robinson P, Redwood C, Watkins H.** Dilated cardiomyopathy mutations in three thin filament regulatory proteins result in a common functional phenotype. *J Biol Chem* 280: 28498–28506, 2005.
36. **Morimoto S, Lu QW, Harada K, Takahashi-Yanaga F, Minakami R, Ohta M, Sasaguri T, Ohtsuki I.** Ca(2+)-desensitizing effect of a deletion mutation Delta K210 in cardiac troponin T that causes familial dilated cardiomyopathy. *Proc Natl Acad Sci USA* 99: 913–918, 2002.
37. **Murphy RT, Mogensen J, Shaw A, Kubo T, Hughes S, McKenna WJ.** Novel mutation in cardiac troponin I in recessive idiopathic dilated cardiomyopathy. *Lancet* 363: 371–372, 2004.
38. **Palmer BM, Fishbaugher DE, Schmitt JP, Wang Y, Alpert NR, Seidman CE, Seidman JG, VanBuren P, Maughan DW.** Differential cross-bridge kinetics of FHC myosin mutations R403Q and R453C in

heterozygous mouse myocardium. *Am J Physiol Heart Circ Physiol* 287: H91–H99, 2004.
39. **Palmiter KA, Tyska MJ, Haeberle JR, Alpert NR, Fananapazir L, Warshaw DM.** R403Q and L908V mutant beta-cardiac myosin from patients with familial hypertrophic cardiomyopathy exhibit enhanced mechanical performance at the single molecule level. *J Muscle Res Cell Motil* 21: 609–620, 2000.
40. **Rayment I, Holden HM, Whittaker M, Yohn CB, Lorenz M, Holmes KC, Milligan RA.** Structure of the actin-myosin complex and its implications for muscle contraction. *Science* 261: 58–65, 1993.
41. **Rayment I, Rypniewski WR, Schmidt-Base K, Smith R, Tomchick DR, Benning MM, Winkelmann DA, Wesenberg G, Holden HM.** Three-dimensional structure of myosin subfragment-1: a molecular motor. *Science* 261: 50–58, 1993.
42. **Sata M, Ikebe M.** Functional analysis of the mutations in the human cardiac beta-myosin that are responsible for familial hypertrophic cardiomyopathy. Implication for the clinical outcome. *J Clin Invest* 98: 2866–2873, 1996.
43. **Schmitt JP, Debold EP, Ahmad F, Armstrong A, Frederico A, Conner DA, Mende U, Lohse MJ, Warshaw D, Seidman CE, Seidman JG.** Cardiac myosin missense mutations cause dilated cardiomyopathy in mouse models and depress molecular motor function. *Proc Natl Acad Sci USA* 103: 14525–14530, 2006.
44. **Schmitt JP, Kamisago M, Asahi M, Li GH, Ahmad F, Mende U, Kranias EG, MacLennan DH, Seidman JG, Seidman CE.** Dilated cardiomyopathy and heart failure caused by a mutation in phospholamban. *Science* 299: 1410–1413, 2003.
45. **Schmitt JP, Kamisago M, Asahi M, Li GH, Ahmad F, Mende U, Kranias EG, MacLennan DH, Seidman JG, Seidman CE.** Dilated cardiomyopathy and heart failure caused by a mutation in phospholamban. *Science* 299: 1410–1413, 2003.
46. **Seidman JG, Seidman C.** The genetic basis for cardiomyopathy: from mutation identification to mechanistic paradigms. *Cell* 104: 557–567, 2001.
47. **Toyoshima YY.** How are myosin fragments bound to nitrocellulose film? *Adv Exp Med Biol* 332: 259–265, 1993.
48. **Tyska MJ, Hayes E, Giewat M, Seidman CE, Seidman JG, Warshaw DM.** Single-molecule mechanics of R403Q cardiac myosin isolated from the mouse model of familial hypertrophic cardiomyopathy. *Circ Res* 86: 737–744, 2000.
49. **Villard E, Duboscq-Bidot L, Charron P, Benaiche A, Conraads V, Sylvius N, Komajda M.** Mutation screening in dilated cardiomyopathy: prominent role of the beta myosin heavy chain gene. *Eur Heart J* 26: 794–803, 2005.
50. **Visscher K, Schnitzer MJ, Block SM.** Single kinesin molecules studied with a molecular force clamp. *Nature* 400: 184–189, 1999.
51. **Volkmann N, Hanein D, Ouyang G, Trybus KM, DeRosier DJ, Lowey S.** Evidence for cleft closure in actomyosin upon ADP release. *Nat Struct Biol* 7: 1147–1155, 2000.
52. **Wang Q, Moncman CL, Winkelmann DA.** Mutations in the motor domain modulate myosin activity and myofibril organization. *J Cell Sci* 116: 4227–4238, 2003.
53. **Warshaw DM.** The in vitro motility assay: a window into the myosin molecular motor. *News Physiol Sci* 11: 1–7, 1996.
54. **Work SS, Warshaw DM.** Computer-assisted tracking of actin filament motility. *Anal Biochem* 202: 275–285, 1992.
55. **Yamashita H, Tyska MJ, Warshaw DM, Lowey S, Trybus KM.** Functional consequences of mutations in the smooth muscle myosin heavy chain at sites implicated in familial hypertrophic cardiomyopathy. *J Biol Chem* 275: 28045–28052, 2000.